Coastal Engineering 64 (2012) 16–25

Contents lists available at SciVerse ScienceDirect

Coastal Engineering

journal homepage: www.elsevier.com/locate/coastaleng

Modal analysis of semi-enclosed basins

Giorgio Bellotti [a,*], Riccardo Briganti [b], Gian Mario Beltrami [c], Leopoldo Franco [a]

[a] Dipartimento di Scienze dell'Ingegneria Civile (DSIC), Università di Roma Tre, via Vito Volterra 62, 00146, Rome, Italy
[b] Division of Infrastructures and Geomatics, University of Nottingham, NG7 2RD Nottingham, UK
[c] Laboratorio Ingegneria Ambientale e Marittima, University of L'Aquila, L'Aquila, Italy

ARTICLE INFO

Article history:
Received 4 August 2011
Received in revised form 30 January 2012
Accepted 6 February 2012
Available online 6 March 2012

Keywords:
Tsunamis
Eigenvalue
Eigenmode
Normal mode
Quasi-normal mode
Finite element method
Resonance
Harbour resonance
Marina di Carrara harbour
Open boundary conditions

ABSTRACT

This paper presents a novel technique for the computation of eigenvalues and eigenvectors of partially enclosed basins such as harbours and bays. The procedure makes use of the finite element approximation of the linear shallow water equations, and converts the time-depending problem into an eigenvalues one. The main point of novelty of this research is the mathematical condition used at the boundary that separates the computational domain from the open sea. While classical techniques impose a zero surface elevation (i.e. a nodal line), here an approximate radiation condition is applied. The use of a radiation condition at the open boundary gives a quadratic eigenvalue problem that admits as solution complex eigenvalues and eigenvectors, thus describing the flow in terms of both standing and progressive waves. The new method is applied to an idealized long and narrow harbour, for which an analytical solution of long wave resonance exists, and to the harbour of Marina di Carrara (Italy), for which measurements and previous numerical computation results are available. In both cases the results show good agreement with the available data.

1. Introduction

Transient forcings of long waves in the coastal areas, such as storms and tsunamis, can excite the natural modes of semi-enclosed basins. This can result in resonance conditions that can induce large amplifications of long waves, increasing coastal hazards and flooding risk. As a consequence, the study of the free and forced oscillations of harbours and bays has a prominent role in Coastal Engineering. The knowledge of the properties of free oscillations of the water surface in a basin is also useful as it allows to identify the locations where larger oscillations can be expected (see Kowalik and Murty, 1993; Sobey, 2006).

A possible approach to identify the frequencies of the natural oscillations is that of reproducing the propagation of waves, from offshore into the basin, using a suitable numerical model. By performing several computations, varying the frequency (and possibly the direction) of the incoming waves, it is then possible to build the amplification diagram. This is defined as the variation, over the wave frequency, of the ratio between the wave height at some points inside the harbour and the height of the incoming waves (sometimes it is used half the ratio). The peaks of the amplification diagram can then be assumed to represent natural oscillation modes, and the corresponding modal shape and frequencies can be deduced. Both linear (Bellotti, 2007; Mei, 1990) and non-linear models (Losada et al., 2004; Shi et al., 2003; Woo and Liu, 2004) can be used, and the reproduced sea state can be either regular or random (Lee et al., 2003).

A more direct approach is to compute the natural oscillations by solving the eigenvalue problem associated to the homogeneous linear shallow water equations, as done by Rao (1966), Sobey (2006), Beltrami et al. (2003) and Beltrami and Bargagli (2005) among others. This is derived by assuming harmonic solutions of the equations, which leads to a boundary value problem in the spatial variables only. In the past two types of boundary conditions have been used: fully reflective conditions has been prescribed along solid boundaries, while a zero surface elevation (i.e. a nodal line) has been imposed at the open sea boundary. Both types of boundary conditions are "adiabatic", i.e. no energy is exchanged across these boundaries. Under these conditions the boundary value problem is of the Sturm–Liouville type. Therefore, the eigenvalues and the eigenvectors are real and describe the flow in terms of purely standing waves. The eigenvectors form an orthogonal basis, hence they are often referred as "normal modes". This property allows to describe a forced system as an expansion of these modes with time-dependent coefficients (see Kowalik and Murty, 1993).

* Corresponding author. Tel.: +39 06 0657333323; fax: +39 06 57333441.
E-mail address: bellotti@uniroma3.it (G. Bellotti).

0378-3839
doi:10.1016/j.coastaleng.2012.02.002

Few analytical solutions have been obtained for simply shaped basins (see Rabinovich, 2009); numerical solutions of the boundary value problem are needed for real basins. The choice of the location of the offshore nodal line has to be done a priori. As it will be better specified in this paper, this is a drawback of the procedure, since it implies to impose the length of those waves with flow across the offshore boundary. Among others, Lee (1971) states that the slope of the water surface at the entrance of the harbour should not be imposed a priori, but should be considered part of the solution itself. Several strategies have been used in the past to overcome these limitations in the computation of natural frequencies. In particular, Butcher and Gilmour (1987) included in the computational domain a very large portion of the ocean, in order to minimise the effect of the offshore nodal line.

A further, alternative approach, is that by Tolkova and Power (2011), who computed the natural modes and frequencies of two natural bays, by applying the Empirical Orthogonal Function analysis to the results of tsunamis simulations. The comparison with experimental data suggests good performance of their method.

In the present paper we propose to remove the constraint of a nodal line at the offshore boundary by using an approximate radiation condition. As it is known, this condition states that waves radiate towards infinity (after reflection at the coast and/or at the basin/harbour boundaries) and the wave energy leaves the computational domain (radiation damping). As it will be shown later on in the present paper, the resulting eigenvalue problem is quadratic, and is similar to that obtained in Structural Dynamics when viscous damping is considered (see He and Fu, 2001). Analogous eigenvalue problems have also been extensively studied in the context of astrophysics (see Kokkotas and Schmidt, 1999), although with reference to the Schrödinger equation. The resulting problem admits complex eigenvalues and eigevectors, thus describing both standing and progressive waves. The eigenvectors are not perfectly orthogonal to each other, so that are sometimes also referred to as "quasi-normal" modes. To the knowledge of the authors, eigenanalysis of semi-enclosed water bodies including radiation damping, has not been previously applied in the context of Coastal Engineering.

The paper is structured as follows. The next section describes the mathematical/numerical procedure. Then the resonance of an idealised long and narrow harbour, for which the analytical solution by Mei (1990) is available, is studied. Then, modal analysis of the harbour of Marina di Carrara, Italy, is carried out. The results are compared with available field measurements of harbour resonance, presented by Bellotti and Franco (2011). In the Conclusions of the paper a brief discussion of how the present technique may be of help in the engineering practice is carried out.

2. Description of the numerical model

We start from the homogeneous linear shallow water equations in two dimensions:

$$\frac{\partial \eta}{\partial t}+\frac{\partial (hu)}{\partial x}+\frac{\partial (hv)}{\partial y}=0 \tag{1}$$

$$\frac{\partial u}{\partial t}+g\frac{\partial \eta}{\partial x}=0 \tag{2}$$

$$\frac{\partial v}{\partial t}+g\frac{\partial \eta}{\partial y}=0 \tag{3}$$

where η is the water free surface elevation, u, v are the components of the depth averaged horizontal velocity along the x and y horizontal coordinates respectively, g the gravity acceleration, t is the time. Hereinafter derivation will be indicated with subscripts to have a more compact notation. Performing the derivative in time of Eq. (1), and using Eqs. (2) and (3), leads to

$$\eta_{tt}-\nabla gh\nabla \eta=0, \tag{4}$$

that is the classical long waves equation. Purely oscillatory in time solutions are found in traditional modal analysis:

$$\eta=Re\left[X(x,y)e^{-i\omega t}\right] \tag{5}$$

where ω is the real modal frequency and $X(x,y)$ is the real modal spatial structure; i is the imaginary unit. As stated in the Introduction, a set of adiabatic boundary conditions is traditionally applied along the contours of the computational domain, i.e.:

$$\eta_n=0 \tag{6}$$

$$\eta=0, \tag{7}$$

where n is the outgoing normal to boundaries. The condition (6) holds along fully reflective boundaries, while Eq. (7) is a nodal line condition applied along the open sea boundary. Using Eq. (5), the Eq. (4) and the boundary conditions (6), (7) become respectively:

$$\omega^2 X-\nabla gh\nabla X=0 \tag{8}$$

$$X_n=0 \tag{9}$$

$$X=0. \tag{10}$$

Eqs. (8)–(10) represent a Sturm–Liuville boundary value problem in space. This problem admits real solutions for ω and a set of real orthogonal real eigenvectors $X(x, y)$, representing purely standing waves. It should be noted that the square of the modal frequency ω appears into the field Eq. (8), while the boundary conditions are independent from it; the implications of this on the resulting eigenvalue problem will be discussed later on in the present section.

We now formulate the boundary value problem in the case of an open offshore boundary along which a radiation boundary condition is applied. The traditional radiation condition by Sommerfeld (1949) is valid at infinite distance from the scattered waves source. Extensive research (1992; Bayliss et al., 1982, Givoli, 1991; Panchang et al., 2000; Steward and Panchang, 2000; Van Dongeren and Svendsen, 1997; Xu et al., 1996) has been carried out in order to derive an approximate form of such a condition, to be used at the artificial boundary, placed at a finite distance from the scattering source, that separates the actual computational domain from the semi-infinite sea. Here the following approximate first order condition is applied:

$$\left(\frac{\partial}{\partial n}+\frac{1}{C}\frac{\partial}{\partial t}+\frac{1}{2R}\right)\eta=0, \tag{11}$$

where $C=\sqrt{gh}$ is the wave celerity in the shallow water approximation. The open boundary is assumed to be a circular sector of radius R centred on the source of scattered/radiating waves. It is to be noted that the present approach differs from the classical methods based on the simulation of waves coming from offshore and propagating into partially closed basins or harbours. In those methods it is possible to decompose the wave field into incident, reflected and scattered waves (Mei, 1990). Here on the contrary no waves incoming from the sea are reproduced, but rather free oscillations of unforced waves are modeled. These oscillations generate a system of scattered waves that radiates toward the semi-infinite sea, with a direction mostly orthogonal to the boundaries at which the condition (11) is

applied. In analogy with the classical modal analysis procedure, η is expressed as

$$\eta = Re\left[X(x,y)e^{st}\right] \tag{12}$$

where s is a complex eigenvalue (e.g. He and Fu, 2001, page 125), defined as $s=-\zeta-i\omega$, $X(x, y)$ is the complex spatial structure of the solution. Note that the imaginary part of s represents the angular frequency of the mode, while the real part represents the exponential damping in time. By using the Euler formula it is easy to see that the time dependence of η is $e^{-\zeta t}cos(-\omega t)$. The boundary value problem becomes:

$$s^2X-\nabla gh\nabla X = 0 \tag{13}$$

and the boundary conditions

$$X_n = 0 \tag{14}$$

and:

$$\left(s+\frac{\sqrt{gh}}{2R}\right)X+\sqrt{gh}X_n = 0. \tag{15}$$

Note that the complex eigenvalue s now appears both into the field Eq. (13) and into the radiation boundary condition (15). What is more relevant is that different powers of s are now found in the mathematical problem: as shown in the following this implies that the eigenvalue problem is now quadratic.

The Finite Element Method (FEM) is applied to find an approximate solution of the mathematical problem. Following for example Beltrami et al. (2001) and Bellotti et al. (2003) it is easy to derive the following weak formulation for the problem (Eqs. (8)–(10)), that uses the nodal line at the offshore boundary:

$$0 = \int\int_{\Omega}\left(\nabla vgh\nabla X-v\omega^2X\right)d\Omega; \tag{16}$$

v is a test function that satisfies the essential boundary condition (10) along the offshore boundary, where it is required that $X=0$; Ω represents the computational domain. For the problem represented by Eqs. (13)–(15), that uses the approximate radiation condition along the boundary $\partial\Omega_{rad}$, the weak formulation is:

$$0 = \int\int_{\Omega}\left(\nabla vgh\nabla X+vs^2X\right)d\Omega+\int_{\partial\Omega_{rad}}Xv\sqrt{gh}\left(s+\frac{\sqrt{gh}}{2R}\right)d(\partial\Omega). \tag{17}$$

Usual techniques of FEM (e.g. Reddy, 1984) are used to convert the weak formulations into a linear system of equations. The computational domain is discretized using triangular elements (linear or nonlinear), and a vector $\{X\}$ of the N discrete values of X represent the solution of the problem (N is the number of the nodes). Eq. (16) then can be transformed into the following system (in matrix form):

$$\omega^2[M]\{X\}+[K]\{X\} = 0 \tag{18}$$

while (17) becomes

$$s^2[M]\{X\}+s[C]\{X\}+[K]\{X\} = 0. \tag{19}$$

Note that the matrices $[M]$ and $[K]$ are not identical in the systems (18) and (19). The system (18) is a (non damped) classical linear eigenvalue problem, that admits N real eigenvectors and eigenfrequencies. The system (19), on the other hand, is a damped problem, is quadratic, and admits as solution a set of N complex eigenvectors and eigenvalues in complex conjugate pairs. The matrix form derived so far allows to establish an analogy with Structural Dynamics: $[M]$, $[C]$ and $[K]$ can be seen respectively as the mass, damping and stiffness matrices of a general time-marching mathematical problem (He and Fu, 2001). The damping matrix $[C]$ is here related to the effects of the radiation condition applied at the offshore boundary $\partial\Omega_{rad}$. As already stated, wave energy is not dissipated, but it is radiated away from the computational domain (Mei, 1990), in agreement with the complex nature of the solution of the eigenproblem (19).

It is interesting to point out some physical interpretations of the complex and real eigenvectors. As clearly described by He and Fu (2001), each point of the complex eigenvector $\{X\}$, solution of the problem (19), has a different phase; this implies that the surface elevation will pass through the zero (equilibrium) level not at the same time, as for (partially) progressive waves. Therefore the nodal points are not fixed. On the contrary, real eigenvectors (as those of the solution of the system (18)) represent oscillations that are perfectly in phase. In this case the surface elevation will pass through the zero level at the same time, and it is certainly possible to state that nodal lines exist. A further relevant difference is that eigenvectors of Eq. (18) are orthogonal, while those of Eq. (19) are not.

3. Applications

3.1. A long and narrow harbour

The investigated harbour is 0.30 m long, 0.06 m wide, and 0.01 m deep (see Fig. 1). It is similar to that used by Madsen (1987) and Bellotti et al. (2003), although the water depth differs from those computations; here we consider a depth such that the lowest order modes are very long waves. The walls of the harbour are fully reflective and its entrance is located along a straight fully reflective coast.

An analytical solution for this simple harbour configuration was presented by Mei (1990). The solution, based on the linear wave theory, is provided in terms of the wave amplification factor $C_a=\frac{1}{2}\frac{H_P}{H_{inc}}$, where H_P is the wave height measured at point P in Fig. 1 and H_{inc} is the incoming wave height. C_a is expressed as:

$$C_a(\omega) = \frac{1}{|Z|}, \tag{20}$$

where Z is the bay impedance given by:

$$Z = cos(kL)+(2k\alpha/\pi)sin(kL)ln(2\gamma k\alpha/\pi e)-ik\alpha sin(kL). \tag{21}$$

with k the wave number, L and 2α respectively the harbour length and width, and $\gamma=1.78107248$. The amplification factor is plotted against the angular frequency in Fig. 2. It can be seen that, for some resonant frequencies, C_a is very large. We assume that the eigenfrequencies of the dynamic system are given by those values of ω at which C_a presents relative maxima.

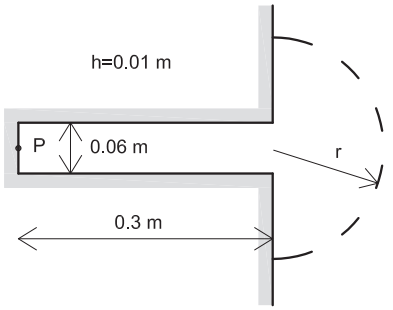

Fig. 1. Sketch of the long and narrow bay; the dashed line represents the offshore boundary, that separates the computational domain from the semi-infinite sea. The amplification diagram reported in Fig. 2 is calculated at the point P.

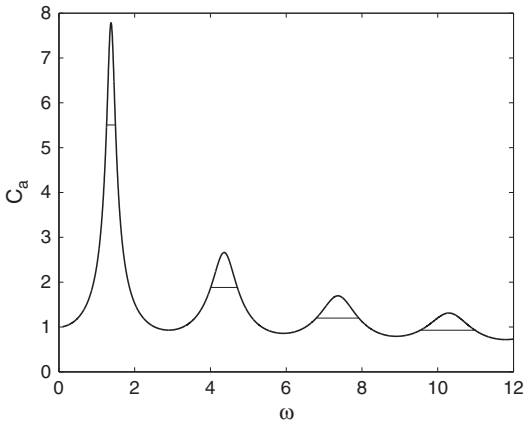

Fig. 2. Amplification diagram of the long and narrow harbour according to the analytical solution by Mei (1990). Horizontal line indicates half power bandwidth for each of the four modes considered.

The analytical solution takes into account the radiation damping. Therefore, as already stated, the waves are free to propagate towards the semi-infinite sea after reflection at the solid boundaries. As discussed by Bellotti (2007), an estimate of the damping factor ζ_n (for each mode n), can be obtained from the amplification factor diagram of Fig. 2. Using simple concepts from the theory of one-dimensional resonators (and under the hypothesis that the damping factor is much smaller than one), it can be shown that $\zeta_n = \Delta\omega_n/2$, where $\Delta\omega_n$ is the width of the portion of the amplification diagram with values larger than $max(C_a)/\sqrt{2}$ for the mode n. $\Delta\omega_n$ is also referred to as the half-power spectral bandwidth.

The present technique and the classical one that uses the nodal line at the offshore boundary were compared in a series of parametric tests aimed at showing the effect of the radius r of the outer semicircular boundary on the results. In each test, the mesh within the harbour was kept constant. Results are presented in Fig. 3 that shows the angular frequencies of the first four modes of the harbour plotted against r. Each subplot refers to a single mode. The frequencies corresponding to the peaks of the amplification diagram, considered as reference values, are shown by solid horizontal lines.

In the case of the first mode, the computations carried out using either the nodal line at the offshore boundary or the radiation condition are in good agreement with results from the analytical solution. However for the higher modes it appears that the nodal line technique, although providing good estimates, is not very stable, and tends to compute scattered frequencies. For the low order modes (1 and 2) the frequency calculated using the nodal line seems to depend linearly on the radius r of the outer computational domain (for the mode 2 this is evident for $r \leq 0.2$ m). This is due to the fact that using a nodal line as the offshore boundary condition, in turn, forces the length of the standing waves in the cross-shore direction. Assuming a radiation condition does not result in the imposition of the slope and value of the solution at the offshore boundary, and makes it possible to obtain these quantities as part of the solution to be found.

When looking at the Fig. 3 it is clear that the present technique provides some sensible improvement with respect to the classical one that uses the nodal line, in terms of frequencies. It is to be noted that for larger values of r, the accuracy does not increase. On the contrary, when using large values of r the solver finds eigenvalues of the system made of the two basins, i.e. the harbour and the outer domains. The latter becomes very large with respect to the former as r grows. As a guideline to the model application it is our feeling that the dimension of the outer domain should be kept as small as possible, so that the normal modes of the harbour are those more significant in the computation.

Note that the proposed technique (i.e. with the radiation condition), directly produces an estimate of the radiation damping, calculated as the real part of each eigenvalue. The Fig. 4 shows the damping factor for the first four modes. In particular, it compares the results of the computations carried out varying the radius r of the outer computational domain (and using the radiation condition) with the damping factors obtained measuring the width of each

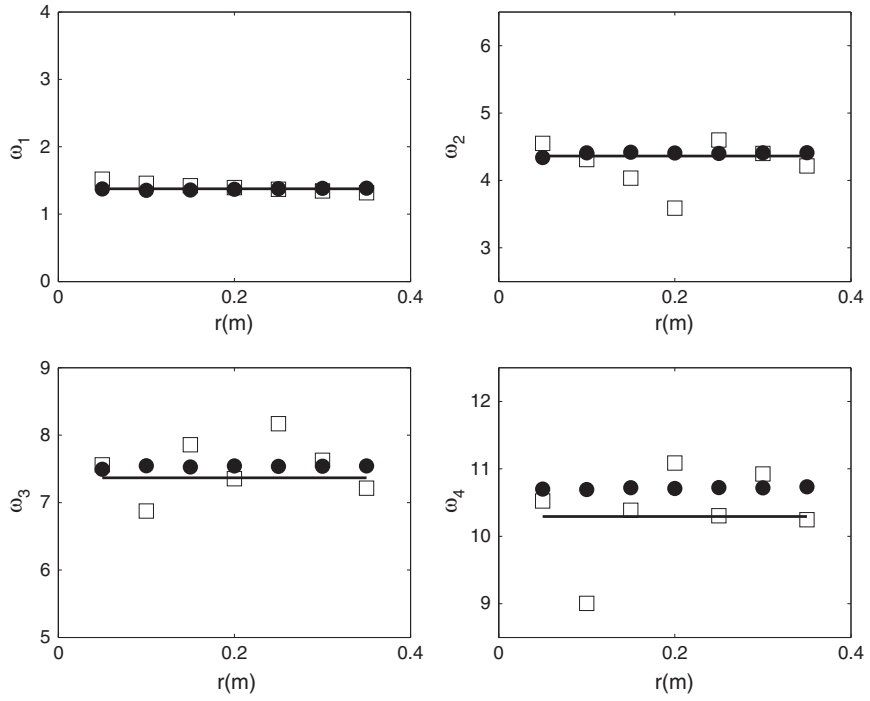

Fig. 3. Angular frequency of the first four modes of the long and narrow harbour. Results of computations carried out varying the radius r of the outer computational domain with the nodal line at the offshore boundary (squares) and with the radiation condition after the iterative process has converged (black dots) are compared against the frequencies derived by the analytical solution by Mei (1990) (horizontal lines).

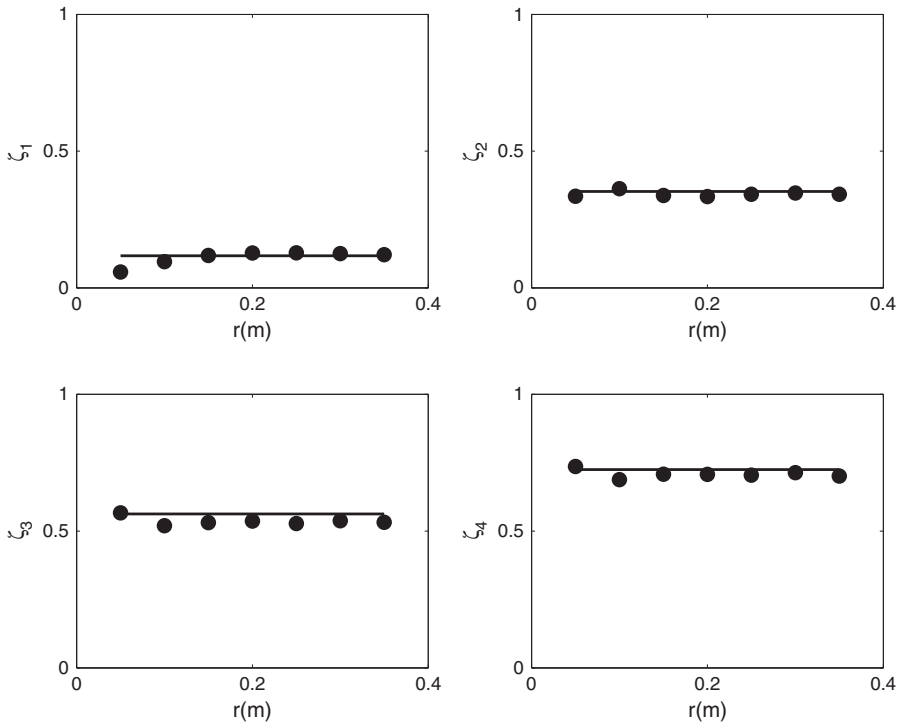

Fig. 4. Damping factors (s^{-1}) of the first four modes of the long and narrow harbour. Results of computations carried out varying the radius r of the outer computational domain using the radiation condition (black dots) are compared with the factors estimated using Mei (1990) analytical solution (solid lines). Note that one of the values of ζ_4 is larger than the limit of the axis of the figure.

peak of the amplification diagram resulting from the analytical solution. There is an overall good agreement between the reference and the calculated values of the damping factor for the four considered modes. However for this parameter it appears that the accuracy of the model results slightly improves with the size of the outer domain.

3.2. Marina di Carrara harbour

The harbour of Marina di Carrara is located along the North-West microtidal Italian coast. The harbour basin has an almost square, regular planshape (Fig. 5) with a total wet surface of about 362,000 m^2. Field measurements of short and long waves and other meteoceanographic parameters, have been carried out since October 2005 (Melito et al., 2006), in order both to manage the harbour quays, and to collect useful information to support the future expansion of the harbour.

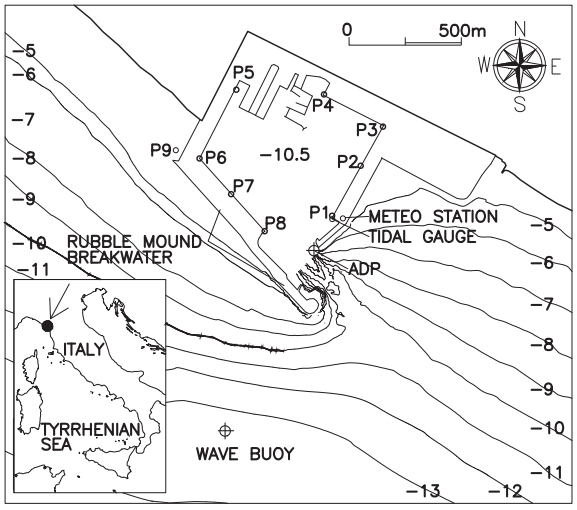

Fig. 5. Plan of harbour of Marina di Carrara and bathymetry, position of pressure sensors (P1–9) and other instruments. The small panel at the bottom left indicates the position of the harbour.

Incoming waves have been recorded by a directional wave buoy (Datawell Waverider), located around 1 km offshore the harbour entrance, at a water depth of 13.5 m. The buoy provides short wave conditions with a time interval of 30 min. Furthermore, a current meter and a pressure transducer are installed at the same location of the buoy in order to measure currents and long waves. Long waves inside the harbour are measured by 8 pressure transducers. The location of each of these devices is shown in Fig. 5, where the sensors are numbered from P1 to P8 starting from the harbour entrance in counterclockwise direction. An additional pressure transducer is located outside the harbour basin at the breakwater (P9). The data, collected at a sampling frequency of 2 Hz, are stored in 1 day long bursts. Further instruments installed in the harbour are: a tidal gauge and a side-looking horizontal acoustic-doppler current-profiler located at the harbour entrance. Finally, a meteorological station is used to measure both the wind velocity and direction, the atmospheric pressure and the air temperature.

Analysis of the measurements has been presented in previous papers. Cuomo et al. (2007) and Melito et al. (2007) discussed, by coupling field measurements and linear/non-linear numerical model results, non-stationarity and non-linearity of harbour resonance. Recently Bellotti and Franco (2011) carried out analysis of three years of records (December 2005–October 2008) of the pressure transducers located inside the harbour. Among other analyses they have presented frequency spectra of the 100 more energetic sea states, and numerical computations to evaluate the amplification diagram of long waves.

As far as the frequency spectra are concerned, Bellotti and Franco (2011) firstly converted the pressure records to surface elevation time series. Then they have divided the one-day bursts into 12 records, each covering 2 h. A frequency spectrum of each 2-hour record,

was obtained using the Fast Fourier Transform. Furthermore, each spectrum was smoothed by means of a moving average filter. The procedure was applied to the signal recorded by all the pressure transducers. Each spectrum was divided into two frequency bands. The first band (f<0.003 Hz) was referred to Very Long Waves (VLW), while the second one (0.003<f<0.030 Hz) to Long Waves (LW). The significant wave height was calculated for each of the two frequency bands, by integrating the energy density over the appropriate frequencies. The significant wave heights, calculated on the basis of the LW frequency band, were arranged in descending order, making it possible to select the first 100 more energetic records.

In order to compare the spectral shape at each pressure transducer, the wave spectra given by the Fourier Transform were normalized with respect to the significant wave height. The normalization was carried out by keeping separate the VLW and LW frequency bands, i.e. for each band it was used the appropriate wave height. When comparing the 100 more energetic normalized spectra of each

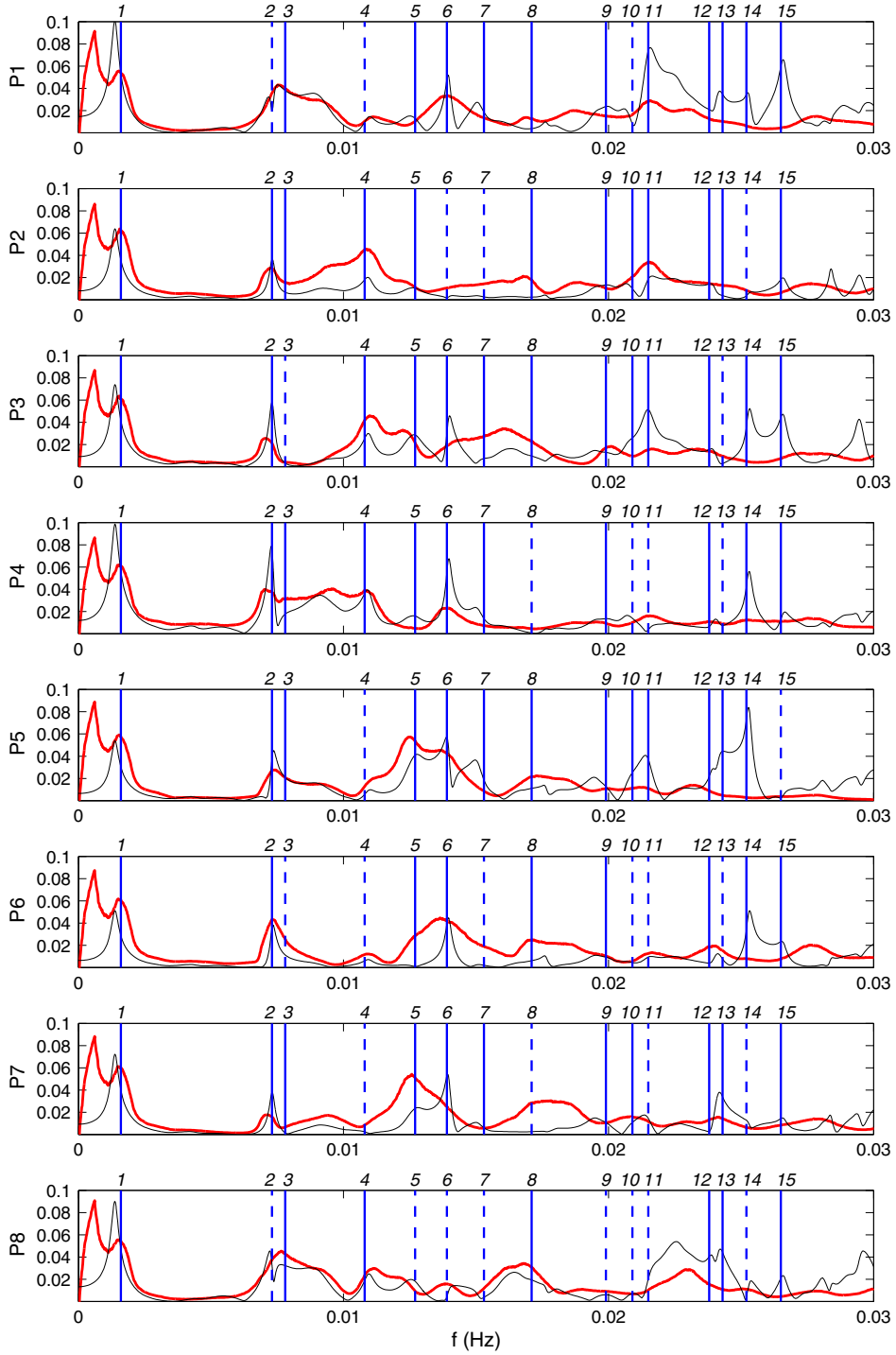

Fig. 6. Eigenfrequencies of the Carrara harbour (vertical blue lines) computed using the radiation condition, compared against the normalized experimental average spectra (red lines) and the amplification diagram obtained by numerical model (black lines). Each panel refers to a pressure gauge, indicated by the number at the y label. Note that the quantity reproduced for each spectra is the amplitude of the Fourier Transform normalized using the significant wave height and is, therefore, nondimensional.

pressure transducer, Bellotti and Franco (2011) found them to be very similar, suggesting that they have always the same shape. This made it possible to calculate a single average spectrum for each pressure transducer. It is to be noted that Maa et al. (2011) recently have drawn similar conclusions analyzing resonance at a harbour in Taiwan.

The average spectra corresponding to the 8 pressure transducers located in the inner harbour of Marina di Carrara are shown in the Fig. 6 by red solid lines. The spectra have several peaks, that can reasonably be considered to correspond to the eigenmodes of the harbour. In the present study a frequency representing these modes has been estimated at the peaks that are evident and sharp. Table 1 reports these frequencies, specifying (superscripts) the pressure gauges used for their estimation.

Bellotti and Franco (2011) also compared the analysis to the results of numerical computations, performed using a linearized equations wave model based on the Mild Slope Equation (Bellotti et al., 2003). By performing many computations of the wave penetration into the harbour, they have built the amplification diagram at the position of the 8 pressure transducers located inside the harbour. The computations were carried out without bottom friction and for a direction of the incoming waves identical to the dominant direction of the short waves, i.e. from South-West. The wave frequency was varied in a wide range between 0.0001 Hz and 0.03 Hz. The amplification diagrams are reported in Fig. 6 using solid black lines. It is worth to stress that the amplification diagrams were built using incoming wave height of unit height, and that they were scaled arbitrarily in order to compare their shape with the experimental ones. Using unit height coincides with assuming that the spectrum of the incoming long waves is rectangular, i.e. constant over the frequency. Also the numerical amplification diagram shows several peaks, most of these in good agreement with the experimental ones. Frequencies of the peaks of the amplification diagram, are reported in the Table 1, specifying as before (superscripts) the location of the pressure gauges used for their estimation.

Eigenmodes of the harbour have been calculated using the computational domain shown in the Fig. 7. At the artificial boundary that separates the harbour from the sea, it has been first applied the nodal line condition, and then the radiation one, in order to compare the results. As for the rectangular harbour the offshore boundary is a circular sector centred on the harbour entrance. For the computational domain shown in the figures the radius of the circular sector used is 160 m.

Table 1
Frequencies (Hz) of the eigenmodes of the Marina di Carrara harbour, as computed by the present numerical model using the nodal line and the radiation condition at the offshore boundary; frequency of the peaks of the experimental spectra and of the amplification diagram of Bellotti and Franco (2011). Superscripts indicate what gauges have been used to estimate the frequency of each mode.

Mode number	Freq. estimated by the nodal line	Freq. estimated by the rad. cond.	Freq. estimated by the exp. spectra	Freq. estimated by the num. res.
1	0.0016	0.0014	$0.0015^{1,3}$	0.0014^{1-8}
2	0.0073	0.0073	$0.0072^{2,3,5}$	0.0073^{1-8}
3	0.0078	0.0079	0.0077^{8}	0.0076^{8}
4	0.0108	0.0107	0.0109^{2}	$0.0109^{1-4,6,8}$
5	0.0127	0.0130	$0.0125^{5,7}$	$0.0126^{1-5,7,8}$
6	0.0139	0.0139	0.0136^{6}	$0.0140^{1,3-7}$
7	0.0153	0.0151	–	$0.0150^{1,4,5,7}$
8	0.0171	0.0170	$0.0169^{1,2}$	–
9	0.0199	0.0198	0.0201^{3}	$0.0199^{1,2,4}$
10	0.0209	0.0207	–	$0.0207^{2,4}$
11	0.0215	0.0215	$0.0216^{1,2,4}$	$0.0215^{1,3,5,7}$
12	0.0238	0.0239	0.0240^{6}	$0.0239^{2,3,8}$
13	0.0243	0.0242	–	$0.0242^{1,7,8}$
14	0.0252	0.0252	–	$0.0253^{1,3-6,8}$
15	0.0265	0.0265	–	$0.0266^{1,2,4,6-8}$

Eigenfrequencies are summarized in the Table 1, and are represented in the Fig. 6 using vertical blue lines. The corresponding eigenmodes are shown in the Fig. 8, where the position of the 8 pressure transducers is shown using small black circles. There the mass normalized absolute value of each mode has been plotted. In order to make easier the following analysis, for each eigenmode it has been evaluated whether or not some of the pressure transducers are expected to measure small surface elevation. For example, referring to the eigenmode 6, it is clear that transducers 1 and 3 are at the position of crest and trough, while transducer 2 can hardly detect this mode, being at the quasi-nodal line. Finally in Fig. 6, an eigenfrequency is plotted using a dashed line in the case that the transducer is at a quasi-nodal line, while a solid line is used in the case that it is expected to measure large surface elevation. In the following each relevant mode is analyzed, and the corresponding eigenfrequency compared with the experimental and the numerical results of Bellotti and Franco (2011). Note that we often use terms like "quasi-standing" waves and "quasi-nodal" lines. This is done in analogy with the definition of "quasi-normal" modes given by Kokkotas and Schmidt (1999).

Mode 1 is the Helmoltz mode of the harbour. The surface elevation is in phase, almost constant in the inner harbour. The computed frequency for this mode is in very good agreement with that desumed by the field measurements, while it appears that the numerical model results by Bellotti and Franco (2011), slightly underestimate the frequency.

Modes 2 and 3 are "quasi-standing" waves inducing minimum surface elevation along the diagonals of the harbour. A trough will be on one side of the harbour when a crest is on the other side. The eigenfrequencies of mode 2 resulting from the calculation carried out imposing either a nodal line or the radiation condition are coincident (see Table 1). Mode 2 has the minimum surface elevation at the harbour entrance; the corresponding mode calculated with the nodal line technique, not represented in the figure, shows a nodal line at the entrance. As shown by Bellotti (2007), this mode tends to be more trapped in the basins with respect to mode 3, that has an antinode near the entrance and therefore is able to generate radiating waves. This is also explained by the damping factors. In fact, while the damping factor of mode 2 ($\zeta = 0.000139$) is of the order of 10^{-4}, that of mode 3 ($\zeta = 0.003639$) is of the order of 10^{-3}. Due to the almost square planshape of the harbour, the frequencies of these modes are very similar. By comparing these eigenfrequencies with the experimental data, it can be desumed that mode 2 is more likely excited, or has larger amplification coefficients than mode 3. The peaks in the spectra pertaining to these frequencies are however quite broad. Therefore, it is reasonable to assume that both modes contribute to the surface oscillations at these frequencies. However the peak frequencies of most of the pressure gauges suggests that mode 2 is more important. This does not apply for the gauges 1 and 8, that for mode 2 are in areas of small amplification.

Mode 4 appears to be dominated by a quasi-standing wave at the North-East boundary of the harbour. The analysis of the corresponding eigenmode suggests that maxima of surface elevation should be observed at gauges 4 and 3, while smaller but still detectable elevations should be observed at gauges 2 and 8. This expectation is confirmed by the comparison of the computed frequency of this mode with the corresponding peak in the experimental spectra. Nevertheless, the peak frequency desumed by the measurements appears larger than that computed.

Mode 5 gives very large surface elevations at the gauge 5. Also gauges 3, 6 and 7 are expected to detect waves pertaining to this mode. The corresponding peak frequency of the average spectra is consistent with what expected. Surprisingly at gauge 6, the numerical results obtained by Bellotti and Franco (2011) using the forcing waves, show no amplification, while the experimental results indicate relevant energy around that frequency. The present technique detects the eigenmode.

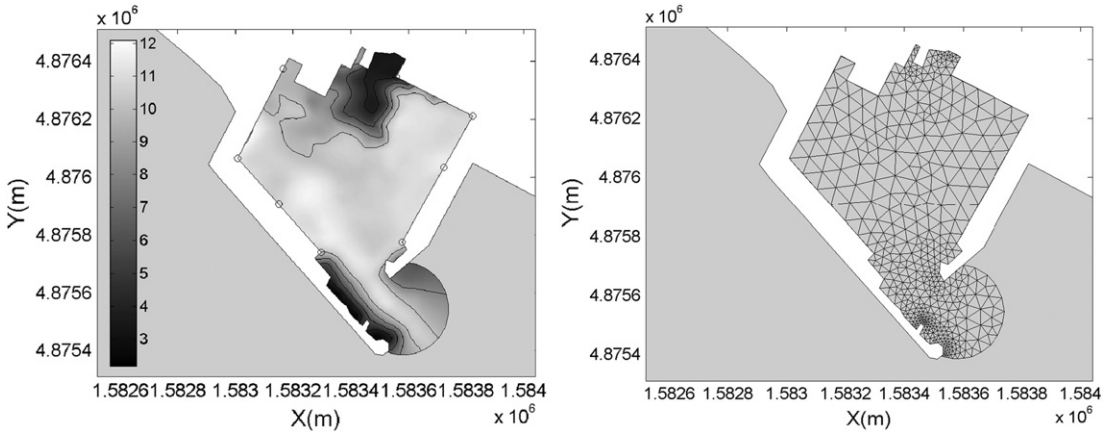

Fig. 7. Marina di Carrara harbour. Left panel: water depth over the computational domain. Right panel: coarse version of the FEM mesh. Note that the offshore boundary is a circular sector centred on the harbour entrance.

Mode 6 appears similar to mode 2, but with two quasi-nodal lines across the diagonal of the harbour. Relevant amplifications are expected at nodes 1, 3, 4, 5, 6. The experimental spectra show peaks around these frequencies for gauges 1, 4, 5, 6. Some energy is also present at gauge 3, but there is not a clear peak in the corresponding average spectrum. The numerical amplification diagram by (Bellotti and Franco, 2011) shows for this mode sharp peak with frequencies well in agreement with those found with the present technique.

Mode 7 gives large amplifications around gauges 4 and 5; however no peaks around this frequencies are found in the measurements.

Mode 8 induces a quasi-standing wave along the North-West boundary of the harbour, between gauges 5 and 6. The spectra show for these gauges quite broad peaks, with frequencies similar to that given by the numerical model. Small peaks are detectable also for gauges 1 and 2, for which the numerical results predict large wave amplitudes. A relevant peak is also clear for the gauge 8, although the peak frequency is smaller than that from the numerical calculation.

As far as mode 9 is concerned, it is possible to identify a peak in the experimental average spectra only at gauge 3. No relevant surface elevation has been measured at gauge 5, although the modal shape predicts large amplitudes at that point. The numerical results show some amplifications for the corresponding frequency only at gauge 1.

Modes 10 and 11 have very similar frequencies and modal shapes. Mode 10 appears to induce larger waves at the North-West side (i.e. between gauges 5 and 6), while mode 11 predicts larger waves at the North-East side of the harbour. The damping factors show the same order of magnitude. Peaks around these frequencies are found in the experimental spectra at gauges 1, 2, 3, and 4. The frequencies of these peaks suggest that mode 11 is more energetic than the 10.

For the modes from 12 to 15 it is not easy to find peaks in the experimental spectra. The results are however in reasonable agreement with the numerical computations carried out by Bellotti and Franco (2011), that show sharp peaks at frequencies compatible with those derived with the present method.

To conclude it appears that modal analysis of the harbour of Marina di Carrara has provided results well in agreement with available analyses of field data and numerical modelling.

4. Conclusions

We have presented a FEM model for the computation of eigenmodes and eigenfrequencies of partially enclosed basins such harbours and bays. The novelty of the model is the treatment of the mathematical condition used at the boundary that separates the computational domain from the open sea. While the classical approach is that of imposing a nodal line at that boundary, requiring the surface elevation to be zero, here a suitable radiation condition has been applied. This allows to reproduce the effects of the radiation damping on the free oscillations of the water surface in the basin. The most important practical consequence of this is that it is possible to estimate the damping factor of the natural modes of the basin. This is an indicator of the degree of trapping of each mode, and of the persistence of the free water surface oscillations inside the basin.

The method was applied to an idealized long and narrow harbour, for which the analytical solution by Mei (1990) is available. Comparison of the analytical solution with the results obtained using the nodal line and the radiation condition, suggests that the new method based on the radiation condition gives some improvements with respect to the classical one, since eigenfrequencies of the harbour appear more accurate. Furthermore it shows that the estimate of the radiation damping is fairly accurate, especially for the two lowest order modes.

The application of the method to the harbour of Marina di Carrara was also successful, since comparison with available experimental data and previous numerical modeling suggests good performance of the present modal analysis technique. However, for this latter test, the difference between the use of the nodal line and the radiation condition in terms of modal frequencies is modest. This is also a consequence of the shape of the harbour, that has a relatively small entrance, inducing a small radiation damping. Nevertheless the use of the radiation condition has the relevant advantage of allowing the calculation of the damping factor. Furthermore we believe that, despite the real part of the eigenfrequencies provided by the two methods are similar, the modal shapes (e.g. the eigenvectors) calculated by the new method that uses the radiation condition (i.e. a condition that makes it possible to describe the wave field in terms of both standing and progressive waves), are more realistic than those given by the classical one that uses a nodal line at the offshore boundary (i.e. a method that inherently describes the wave field in terms of purely standing waves, given the real value of the solution).

We believe that modal analysis of harbours, with the improvement of the radiation condition at the offshore boundary, is a useful tool to support engineering practice. In fact the computation of the eigenmodes easily allows to identify the areas/points of the basin that are expected to experience large surface oscillations, and the frequency of the long waves that can resonate inside the harbour. However the model presented in this paper is not alternative to the methods used for the computation of the amplification diagram as that used by Bellotti and Franco (2011). Given the theory and the numerics developed so far, the present method allows identification of modal shapes and frequencies, but not amplifications. It is also worth to remember that in the practice it is important to look not only at the response of the basin, i.e. how it would react when forced by long waves of given frequencies, but also at the forcing long waves

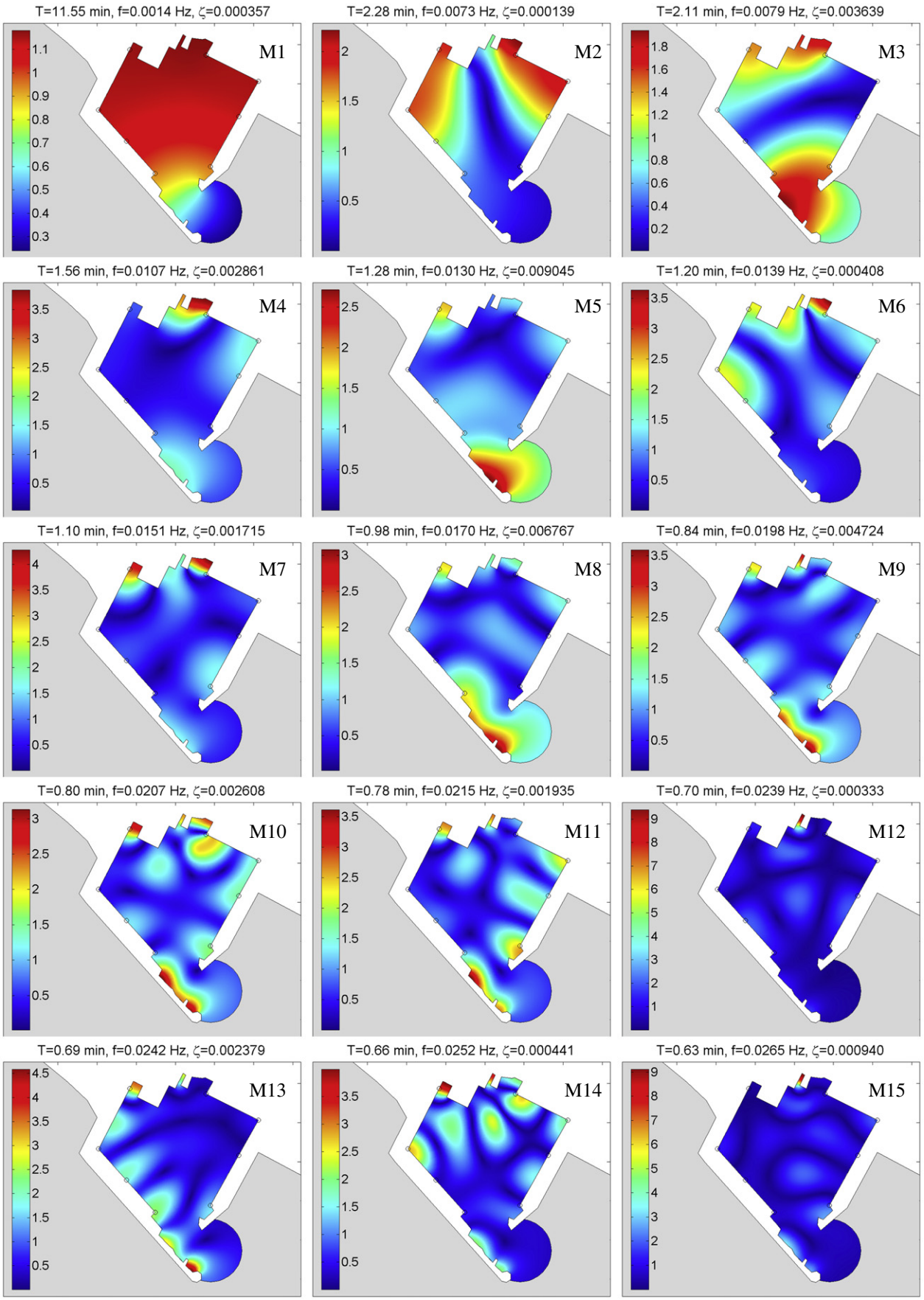

Fig. 8. Eigenmodes of the Carrara harbour computed using the radiation condition. The mass normalized absolute value of each eigenvector is represented.

(Bellotti and Franco, 2011; Bowers, 1977; De Girolamo, 1996; Madsen and Sørensen, 1993; Stiassnie and Drimer, 2006).

Acknowledgements

This work was partially funded by the Italian Ministry of Research (MIUR), under the research project FIRB 2008-FUTURO IN RICERCA (Design, construction and operation of the Submarine Multidisciplinary Observatory experiment). The measurements at the harbour of Marina di Carrara have been carried out within the framework of a research project carried out at the University of Rome Tre, and funded by the Port Authority of Marina di Carrara. The authors thank Dr. I. Melito (Port Authority of Marina di Carrara) for providing the data and for the support to this research. R. Briganti would like to express his gratitude to the EPSRC for supporting him through a Career Acceleration Fellowship (EP/1004505/1). We wish to sincerely thank the two anonymous Reviewers. According to one of their useful remarks, we were suggested to use Eq. (11) instead of a simpler condition; this has largely improved the accuracy of the results and the stability of the model.

References

Bayliss, A., Gunzburger, M., Turkel, E., 1982. Boundary conditions for the numerical solution of elliptic equations in exterior regions. SIAM Journal on Applied Mathematics 42 (2), 430–451 URL http://link.aip.org/link/?SMM/42/430/1.

Bellotti, G., 2007. Transient response of harbours to long waves under resonance conditions. Coastal Engineering 54 (9), 680–693.

Bellotti, G., Beltrami, G.M., De Girolamo, P., 2003. Internal generation of waves in 2D fully elliptic mild-slope equation FEM models. Coastal Engineering 49 (1–2), 71–81.

Bellotti, G., Franco, L., 2011. Measurement of long waves at the harbor of Marina di Carrara, Italy. Ocean Dynamics 61, 2051–2059 ISSN: 1616-7341. doi:10.1007/s10236-011-0468-6.

Beltrami, G., Bargagli, A., 2005. Computational improvement of gravitational mode calculation of basins discretised by orthogonal curvilinear grids. Ocean Engineering 32 (13), 1623–1630.

Beltrami, G.M., Bargagli, A., Briganti, R., 2003. Gravitational mode calculation of basin discretised by orthogonal curvilinear grid. Ocean Engineering 30 (7), 833–853.

Beltrami, G.M., Bellotti, G., De Girolamo, P., Sammarco, P., 2001. Treatment of wave-breaking and total absorption in a mild-slope equation FEM model. ASCE Journal of Waterway, Port, Coastal and Ocean Engineering 127 (5), 263–271.

Bowers, E.C., 1977. Harbour resonances due to set-down beneath wave groups. Journal of Fluid Mechanics 79, 71–92.

Butcher, C.N., Gilmour, A.E., 1987. Free oscillations in Wellington and Lyttelton harbours. Tech. Rep. 1(1), DMFS Reports, New Zeland.

Cuomo, G., Franco, L., Melito, I., 2007. Coupled Field Measurements and Numerical Modeling of Harbour Resonance at Marina di Carrara. Ports 2007, Proceedings of the Eleventh Triennial International Conference. ASCE.

De Girolamo, P., 1996. An experiment on harbour resonance induced by incident regular waves and irregular short waves. Coastal Engineering 27 (1–2), 47–66.

Givoli, D., 1991. Non-reflecting boundary conditions. Journal of Computational Physics 94 (1), 1–29.

Givoli, D., 1992. A numerical-solution procedure for exterior wave problems. Computers and Structures 43 (1), 77–84.

He, J., Fu, Z.-F., 2001. Modal Analysis. Butterworth-Heinemann.

Kokkotas, K.D., Schmidt, B.G., 1999. Quasi-normal modes of stars and black holes. Living Reviews in Relativity 2 Online Article.

Kowalik, Z., Murty, T.S., 1993. Numerical modeling of ocean dynamics. Advanced Series on Ocean Engineering, vol. 5. World Scientific, Singapore.

Lee, C., Kim, G., Suh, K.-D., 2003. Extended mild-slope equation for random waves. Coastal Engineering 48 (4), 277–287.

Lee, J.J., 1971. Wave-induced oscillations in harbours of arbitrary geometry. Journal of Fluid Mechanics 45 (2), 375–394.

Losada, I., Liu, P., Gonzalez, M., Diaz, G., Gonzalez, J., Woo, S., 2004. Harbour short wave agitation and resonance based on modified Boussinesq equations. In: Smith, J.M. (Ed.), Proc. 29th Int. Conf. Coastal Eng. ASCE, Lisbon.

Maa, J., Tsai, C.-H., Juang, W.-J., Tseng, H.-M., 2011. A preliminary study on Typhoon Tim induced resonance at Hualien Harbor, Taiwan. Ocean Dynamics 61, 411–423.

Madsen, Larsen, 1987. An efficient finite-difference approach to the mild-slope equation. Coastal Engineering 11, 329–351.

Madsen, P., Sørensen, O., 1993. Bound waves and triad interactions in shallow waters. Ocean Engineering 20, 359–388.

Mei, C.C., 1990. The Applied Dynamics of Ocean Surface Waves, 2nd edition. Advanced Series on Ocean Engineering., vol. 1. World Scientific, Singapore.

Melito, I., Cuomo, G., Bellotti, G., Franco, L., 2006. Field measurements of harbour resonance at Marina di Carrara. In: Smith, J.M. (Ed.), Proc. 30th Int. Conf. Coastal Eng. ASCE, San Diego.

Melito, I., Cuomo, G., Franco, L., Guza, R., 2007. Harbour resonance at Marina di Carrara: linear and non linear aspects. Proceedings of Coastal Structures 2007. ASCE, pp. 1647–1658.

Panchang, V., Chen, W., Xu, B., Schlenker, K., Demirbilek, Z., Okihiro, M., 2000. Exterior bathymetric effects in elliptic harbor wave models. ASCE Journal of Waterway, Port, Coastal and Ocean Engineering 126 (2), 71–78.

Rabinovich, A.B., 2009. Seiches and harbor oscillations. In: Kim, Y.C. (Ed.), Handbook of coastal and ocean engineering. World Scientific Publ., pp. 193–236.

Rao, D., 1966. Free gravitational oscillations in rotating rectangular basins. Journal of Fluid Mechanics 25 (Part 3), 523–555.

Reddy, J., 1984. An introduction to the finite element method. Mathematics and statistics series. McGraw-Hill.

Shi, F., Kirby, J., Dalrymple, R., Chen, Q., 2003. Wave simulations in Ponce de Leon Inlet using Boussinesq model. ASCE Journal of Waterway, Port, Coastal and Ocean Engineering 129 (3), 124–135.

Sobey, R.J., 2006. Normal mode decomposition for identification of storm tide and tsunami hazard. Coastal Engineering 53 (2–3), 289–301.

Sommerfeld, A., 1949. Partial Differential Equations in Physics. Academic Press.

Steward, D.R., Panchang, V.G., 2000. Improved boundary condition for surface water waves. Ocean Engineering 28, 139–157.

Stiassnie, M., Drimer, N., 2006. Prediction of long forcing waves for harbor agitation studies. ASCE Journal of Waterway, Port, Coastal and Ocean Engineering 132 (3), 166–171.

Tolkova, E., Power, W., 2011. Obtaining natural oscillatory modes of bays and harbors via Empirical Orthogonal Function analysis of tsunami wave fields. Ocean Dynamics 61 (6), 731–751.

Van Dongeren, A.R., Svendsen, I.A., 1997. Absorbing-generating boundary condition for shallow water models. ASCE Journal of Waterway, Port, Coastal and Ocean Engineering 123 (6), 303–313.

Woo, S., Liu, P.L., 2004. Finite-element model for modified Boussinesq equations. 1: Model development. ASCE Journal of Waterway, Port, Coastal and Ocean Engineering 130 (1), 1–16.

Xu, B., Panchang, V., Demirbilek, Z., 1996. Exterior reflections in elliptic harbor wave models. Journal of Waterway, Port, Coastal, and Ocean Engineering 122 (3), 118–126.